Observation of $\psi(3686) \rightarrow \Xi(1530)^-\bar{\Xi}(1530)^+$ and $\Xi(1530)^-\bar{\Xi}^+$

M. Ablikim,[1] M. N. Achasov,[10,d] P. Adlarson,[59] S. Ahmed,[15] M. Albrecht,[4] M. Alekseev,[58a,58c] A. Amoroso,[58a,58c] F. F. An,[1] Q. An,[55,43] Y. Bai,[42] O. Bakina,[27] R. Baldini Ferroli,[23a] Y. Ban,[35] K. Begzsuren,[25] J. V. Bennett,[5] N. Berger,[26] M. Bertani,[23a] D. Bettoni,[24a] F. Bianchi,[58a,58c] J. Biernat,[59] J. Bloms,[52] I. Boyko,[27] R. A. Briere,[5] H. Cai,[60] X. Cai,[1,43] A. Calcaterra,[23a] G. F. Cao,[1,47] N. Cao,[1,47] S. A. Cetin,[46b] J. Chai,[58c] J. F. Chang,[1,43] W. L. Chang,[1,47] G. Chelkov,[27,b,c] D. Y. Chen,[6] G. Chen,[1] H. S. Chen,[1,47] J. C. Chen,[1] M. L. Chen,[1,43] S. J. Chen,[33] Y. B. Chen,[1,43] W. Cheng,[58c] G. Cibinetto,[24a] F. Cossio,[58c] X. F. Cui,[34] H. L. Dai,[1,43] J. P. Dai,[38,h] X. C. Dai,[1,47] A. Dbeyssi,[15] D. Dedovich,[27] Z. Y. Deng,[1] A. Denig,[26] I. Denysenko,[27] M. Destefanis,[58a,58c] F. De Mori,[58a,58c] Y. Ding,[31] C. Dong,[34] J. Dong,[1,43] L. Y. Dong,[1,47] M. Y. Dong,[1,43,47] Z. L. Dou,[33] S. X. Du,[63] J. Z. Fan,[45] J. Fang,[1,43] S. S. Fang,[1,47] Y. Fang,[1] R. Farinelli,[24a,24b] L. Fava,[58b,58c] F. Feldbauer,[4] G. Felici,[23a] C. Q. Feng,[55,43] M. Fritsch,[4] C. D. Fu,[1] Y. Fu,[1] Q. Gao,[1] X. L. Gao,[55,43] Y. Gao,[45] Y. Gao,[56] Y. G. Gao,[6] Z. Gao,[55,43] B. Garillon,[26] I. Garzia,[24a] E. M. Gersabeck,[50] A. Gilman,[51] K. Goetzen,[11] L. Gong,[34] W. X. Gong,[1,43] W. Gradl,[26] M. Greco,[58a,58c] L. M. Gu,[33] M. H. Gu,[1,43] S. Gu,[2] Y. T. Gu,[13] A. Q. Guo,[22] L. B. Guo,[32] R. P. Guo,[36] Y. P. Guo,[26] A. Guskov,[27] S. Han,[60] X. Q. Hao,[16] F. A. Harris,[48] K. L. He,[1,47] F. H. Heinsius,[4] T. Held,[4] Y. K. Heng,[1,43,47] Y. R. Hou,[47] Z. L. Hou,[1] H. M. Hu,[1,47] J. F. Hu,[38,h] T. Hu,[1,43,47] Y. Hu,[1] G. S. Huang,[55,43] J. S. Huang,[16] X. T. Huang,[37] X. Z. Huang,[33] N. Huesken,[52] T. Hussain,[57] W. Ikegami Andersson,[59] W. Imoehl,[22] M. Irshad,[55,43] Q. Ji,[1] Q. P. Ji,[16] X. B. Ji,[1,47] X. L. Ji,[1,43] H. L. Jiang,[37] X. S. Jiang,[1,43,47] X. Y. Jiang,[34] J. B. Jiao,[37] Z. Jiao,[18] D. P. Jin,[1,43,47] S. Jin,[33] Y. Jin,[49] T. Johansson,[59] N. Kalantar-Nayestanaki,[29] X. S. Kang,[31] R. Kappert,[29] M. Kavatsyuk,[29] B. C. Ke,[1] I. K. Keshk,[4] T. Khan,[55,43] A. Khoukaz,[52] P. Kiese,[26] R. Kiuchi,[1] R. Kliemt,[11] L. Koch,[28] O. B. Kolcu,[46b,f] B. Kopf,[4] M. Kuemmel,[4] M. Kuessner,[4] A. Kupsc,[59] M. Kurth,[1] M. G. Kurth,[1,47] W. Kühn,[28] J. S. Lange,[28] P. Larin,[15] L. Lavezzi,[58c] H. Leithoff,[26] T. Lenz,[26] C. Li,[59] Cheng Li,[55,43] D. M. Li,[63] F. Li,[1,43] F. Y. Li,[35] G. Li,[1] H. B. Li,[1,47] H. J. Li,[9,j] J. C. Li,[1] J. W. Li,[41] Ke Li,[1] L. K. Li,[1] Lei Li,[3] P. L. Li,[55,43] P. R. Li,[30] Q. Y. Li,[37] W. D. Li,[1,47] W. G. Li,[1] X. H. Li,[55,43] X. L. Li,[37] X. N. Li,[1,43] X. Q. Li,[34] Z. B. Li,[44] Z. Y. Li,[44] H. Liang,[1,47] H. Liang,[55,43] Y. F. Liang,[40] Y. T. Liang,[28] G. R. Liao,[12] L. Z. Liao,[1,47] J. Libby,[21] C. X. Lin,[44] D. X. Lin,[15] Y. J. Lin,[13] B. Liu,[38,h] B. J. Liu,[1] C. X. Liu,[1] D. Liu,[55,43] D. Y. Liu,[38,h] F. H. Liu,[39] Fang Liu,[1] Feng Liu,[6] H. B. Liu,[13] H. M. Liu,[1,47] Huanhuan Liu,[1] Huihui Liu,[17] J. B. Liu,[55,43] J. Y. Liu,[1,47] K. Y. Liu,[31] Ke Liu,[6] Q. Liu,[47] S. B. Liu,[55,43] T. Liu,[1,47] X. Liu,[30] X. Y. Liu,[1,47] Y. B. Liu,[34] Z. A. Liu,[1,43,47] Zhiqing Liu,[37] Y. F. Long,[35] X. C. Lou,[1,43,47] H. J. Lu,[18] J. D. Lu,[1,47] J. G. Lu,[1,43] Y. Lu,[1] Y. P. Lu,[1,43] C. L. Luo,[32] M. X. Luo,[62] P. W. Luo,[44] T. Luo,[9,j] X. L. Luo,[1,43] S. Lusso,[58c] X. R. Lyu,[47] F. C. Ma,[31] H. L. Ma,[1] L. L. Ma,[37] M. M. Ma,[1,47] Q. M. Ma,[1] X. N. Ma,[34] X. X. Ma,[1,47] X. Y. Ma,[1,43] Y. M. Ma,[37] F. E. Maas,[15] M. Maggiora,[58a,58c] S. Maldaner,[26] S. Malde,[53] Q. A. Malik,[57] A. Mangoni,[23b] Y. J. Mao,[35] Z. P. Mao,[1] S. Marcello,[58a,58c] Z. X. Meng,[49] J. G. Messchendorp,[29] G. Mezzadri,[24a] J. Min,[1,43] T. J. Min,[33] R. E. Mitchell,[22] X. H. Mo,[1,43,47] Y. J. Mo,[6] C. Morales Morales,[15] N. Yu. Muchnoi,[10,d] H. Muramatsu,[51] A. Mustafa,[4] S. Nakhoul,[11,g] Y. Nefedov,[27] F. Nerling,[11,g] I. B. Nikolaev,[10,d] Z. Ning,[1,43] S. Nisar,[8,k] S. L. Niu,[1,43] S. L. Olsen,[47] Q. Ouyang,[1,43,47] S. Pacetti,[23b] Y. Pan,[55,43] M. Papenbrock,[59] P. Patteri,[23a] M. Pelizaeus,[4] H. P. Peng,[55,43] K. Peters,[11,g] J. Pettersson,[59] J. L. Ping,[32] R. G. Ping,[1,47] A. Pitka,[4] R. Poling,[51] V. Prasad,[55,43] M. Qi,[33] T. Y. Qi,[2] S. Qian,[1,43] C. F. Qiao,[47] N. Qin,[60] X. P. Qin,[13] X. S. Qin,[4] Z. H. Qin,[1,43] J. F. Qiu,[1] S. Q. Qu,[34] K. H. Rashid,[57,i] C. F. Redmer,[26] M. Richter,[4] M. Ripka,[26] A. Rivetti,[58c] V. Rodin,[29] M. Rolo,[58c] G. Rong,[1,47] Ch. Rosner,[15] M. Rump,[52] A. Sarantsev,[27,e] M. Savrié,[24b] K. Schoenning,[59] W. Shan,[19] X. Y. Shan,[55,43] M. Shao,[55,43] C. P. Shen,[2] P. X. Shen,[34] X. Y. Shen,[1,47] H. Y. Sheng,[1] X. Shi,[1,43] X. D. Shi,[55,43] J. J. Song,[37] Q. Q. Song,[55,43] X. Y. Song,[1] S. Sosio,[58a,58c] C. Sowa,[4] S. Spataro,[58a,58c] F. F. Sui,[37] G. X. Sun,[1] J. F. Sun,[16] L. Sun,[60] S. S. Sun,[1,47] X. H. Sun,[1] Y. J. Sun,[55,43] Y. K. Sun,[55,43] Y. Z. Sun,[1] Z. J. Sun,[1,43] Z. T. Sun,[1] Y. T. Tan,[55,43] C. J. Tang,[40] G. Y. Tang,[1] X. Tang,[1] V. Thoren,[59] B. Tsednee,[25] I. Uman,[46d] B. Wang,[1] B. L. Wang,[47] C. W. Wang,[33] D. Y. Wang,[35] H. H. Wang,[37] K. Wang,[1,43] L. L. Wang,[1] L. S. Wang,[1] M. Wang,[37] M. Z. Wang,[35] Meng Wang,[1,47] P. L. Wang,[1] R. M. Wang,[61] W. P. Wang,[55,43] X. Wang,[35] X. F. Wang,[30,*] X. L. Wang,[9,j] Y. Wang,[55,43] Y. Wang,[44] Y. F. Wang,[1,43,47] Z. Wang,[1,43] Z. G. Wang,[1,43] Z. Y. Wang,[1] Zongyuan Wang,[1,47] T. Weber,[4] D. H. Wei,[12] P. Weidenkaff,[26] H. W. Wen,[32] S. P. Wen,[1] U. Wiedner,[4] G. Wilkinson,[53] M. Wolke,[59] L. H. Wu,[1] L. J. Wu,[1,47] Z. Wu,[1,43] L. Xia,[55,43] Y. Xia,[20] S. Y. Xiao,[1] Y. J. Xiao,[1,47] Z. J. Xiao,[32] Y. G. Xie,[1,43] Y. H. Xie,[6] T. Y. Xing,[1,47] X. A. Xiong,[1,47] Q. L. Xiu,[1,43] G. F. Xu,[1] L. Xu,[1] Q. J. Xu,[14] W. Xu,[1,47] X. P. Xu,[41] F. Yan,[56] L. Yan,[58a,58c] W. B. Yan,[55,43] W. C. Yan,[2] Y. H. Yan,[20] H. J. Yang,[38,h] H. X. Yang,[1] L. Yang,[60] R. X. Yang,[55,43] S. L. Yang,[1,47] Y. H. Yang,[33] Y. X. Yang,[12] Yifan Yang,[1,47] Z. Q. Yang,[20] M. Ye,[1,43] M. H. Ye,[7] J. H. Yin,[1] Z. Y. You,[44] B. X. Yu,[1,43,47] C. X. Yu,[34] J. S. Yu,[20] C. Z. Yuan,[1,47] X. Q. Yuan,[35] Y. Yuan,[1] A. Yuncu,[46b,a] A. A. Zafar,[57] Y. Zeng,[20] B. X. Zhang,[1] B. Y. Zhang,[1,43] C. C. Zhang,[1] D. H. Zhang,[1] H. H. Zhang,[44] H. Y. Zhang,[1,43] J. Zhang,[1,47] J. L. Zhang,[61] J. Q. Zhang,[4] J. W. Zhang,[1,43,47] J. Y. Zhang,[1] J. Z. Zhang,[1,47] K. Zhang,[1,47] L. Zhang,[45] S. F. Zhang,[33] T. J. Zhang,[38,h] X. Y. Zhang,[37] Y. Zhang,[55,43] Y. H. Zhang,[1,43] Y. T. Zhang,[55,43] Yang Zhang,[1] Yao Zhang,[1] Yi Zhang,[9,j] Yu Zhang,[47] Z. H. Zhang,[6] Z. P. Zhang,[55] Z. Y. Zhang,[60] G. Zhao,[1] J. W. Zhao,[1,43] J. Y. Zhao,[1,47] J. Z. Zhao,[1,43] Lei Zhao,[55,43] Ling Zhao,[1] M. G. Zhao,[34] Q. Zhao,[1] S. J. Zhao,[63] T. C. Zhao,[1] Y. B. Zhao,[1,43] Z. G. Zhao,[55,43] A. Zhemchugov,[27,b] B. Zheng,[56] J. P. Zheng,[1,43] Y. Zheng,[35] Y. H. Zheng,[47] B. Zhong,[32]

L. Zhou,[1,43] L. P. Zhou,[1,47] Q. Zhou,[1,47] X. Zhou,[60] X. K. Zhou,[47] X. R. Zhou,[55,43] Xiaoyu Zhou,[20] Xu Zhou,[20] A. N. Zhu,[1,47] J. Zhu,[34] J. Zhu,[44] K. Zhu,[1] K. J. Zhu,[1,43,47] S. H. Zhu,[54] W. J. Zhu,[34] X. L. Zhu,[45] Y. C. Zhu,[55,43] Y. S. Zhu,[1,47] Z. A. Zhu,[1,47] J. Zhuang,[1,43] B. S. Zou,[1] and J. H. Zou[1]

(BESIII Collaboration)

[1]*Institute of High Energy Physics, Beijing 100049, People's Republic of China*
[2]*Beihang University, Beijing 100191, People's Republic of China*
[3]*Beijing Institute of Petrochemical Technology, Beijing 102617, People's Republic of China*
[4]*Bochum Ruhr-University, D-44780 Bochum, Germany*
[5]*Carnegie Mellon University, Pittsburgh, Pennsylvania 15213, USA*
[6]*Central China Normal University, Wuhan 430079, People's Republic of China*
[7]*China Center of Advanced Science and Technology, Beijing 100190, People's Republic of China*
[8]*COMSATS University Islamabad, Lahore Campus, Defence Road, Off Raiwind Road, 54000 Lahore, Pakistan*
[9]*Fudan University, Shanghai 200443, People's Republic of China*
[10]*G.I. Budker Institute of Nuclear Physics SB RAS (BINP), Novosibirsk 630090, Russia*
[11]*GSI Helmholtzcentre for Heavy Ion Research GmbH, D-64291 Darmstadt, Germany*
[12]*Guangxi Normal University, Guilin 541004, People's Republic of China*
[13]*Guangxi University, Nanning 530004, People's Republic of China*
[14]*Hangzhou Normal University, Hangzhou 310036, People's Republic of China*
[15]*Helmholtz Institute Mainz, Johann-Joachim-Becher-Weg 45, D-55099 Mainz, Germany*
[16]*Henan Normal University, Xinxiang 453007, People's Republic of China*
[17]*Henan University of Science and Technology, Luoyang 471003, People's Republic of China*
[18]*Huangshan College, Huangshan 245000, People's Republic of China*
[19]*Hunan Normal University, Changsha 410081, People's Republic of China*
[20]*Hunan University, Changsha 410082, People's Republic of China*
[21]*Indian Institute of Technology Madras, Chennai 600036, India*
[22]*Indiana University, Bloomington, Indiana 47405, USA*
[23a]*INFN Laboratori Nazionali di Frascati, I-00044 Frascati, Italy*
[23b]*INFN and University of Perugia, I-06100 Perugia, Italy*
[24a]*INFN Sezione di Ferrara, I-44122 Ferrara, Italy*
[24b]*University of Ferrara, I-44122 Ferrara, Italy*
[25]*Institute of Physics and Technology, Peace Avenue 54B, Ulaanbaatar 13330, Mongolia*
[26]*Johannes Gutenberg University of Mainz, Johann-Joachim-Becher-Weg 45, D-55099 Mainz, Germany*
[27]*Joint Institute for Nuclear Research, 141980 Dubna, Moscow region, Russia*
[28]*Justus-Liebig-Universitaet Giessen, II. Physikalisches Institut, Heinrich-Buff-Ring 16, D-35392 Giessen, Germany*
[29]*KVI-CART, University of Groningen, NL-9747 AA Groningen, Netherlands*
[30]*Lanzhou University, Lanzhou 730000, People's Republic of China*
[31]*Liaoning University, Shenyang 110036, People's Republic of China*
[32]*Nanjing Normal University, Nanjing 210023, People's Republic of China*
[33]*Nanjing University, Nanjing 210093, People's Republic of China*
[34]*Nankai University, Tianjin 300071, People's Republic of China*
[35]*Peking University, Beijing 100871, People's Republic of China*
[36]*Shandong Normal University, Jinan 250014, People's Republic of China*
[37]*Shandong University, Jinan 250100, People's Republic of China*
[38]*Shanghai Jiao Tong University, Shanghai 200240, People's Republic of China*
[39]*Shanxi University, Taiyuan 030006, People's Republic of China*
[40]*Sichuan University, Chengdu 610064, People's Republic of China*
[41]*Soochow University, Suzhou 215006, People's Republic of China*
[42]*Southeast University, Nanjing 211100, People's Republic of China*
[43]*State Key Laboratory of Particle Detection and Electronics, Beijing 100049, Hefei 230026, People's Republic of China*
[44]*Sun Yat-Sen University, Guangzhou 510275, People's Republic of China*
[45]*Tsinghua University, Beijing 100084, People's Republic of China*
[46a]*Ankara University, 06100 Tandogan, Ankara, Turkey*
[46b]*Istanbul Bilgi University, 34060 Eyup, Istanbul, Turkey*
[46c]*Uludag University, 16059 Bursa, Turkey*
[46d]*Near East University, Nicosia, North Cyprus, Mersin 10, Turkey*
[47]*University of Chinese Academy of Sciences, Beijing 100049, People's Republic of China*

^{48}University of Hawaii, Honolulu, Hawaii 96822, USA

^{49}University of Jinan, Jinan 250022, People's Republic of China

^{50}University of Manchester, Oxford Road, Manchester M13 9PL, United Kingdom

^{51}University of Minnesota, Minneapolis, Minnesota 55455, USA

^{52}University of Muenster, Wilhelm-Klemm-Strasse 9, 48149 Muenster, Germany

^{53}University of Oxford, Keble Road, Oxford OX13RH, United Kingdom

^{54}University of Science and Technology Liaoning, Anshan 114051, People's Republic of China

^{55}University of Science and Technology of China, Hefei 230026, People's Republic of China

^{56}University of South China, Hengyang 421001, People's Republic of China

^{57}University of the Punjab, Lahore-54590, Pakistan

^{58a}University of Turin, I-10125 Turin, Italy

^{58b}University of Eastern Piedmont, I-15121 Alessandria, Italy

^{58c}INFN, I-10125 Turin, Italy

^{59}Uppsala University, Box 516, SE-75120 Uppsala, Sweden

^{60}Wuhan University, Wuhan 430072, People's Republic of China

^{61}Xinyang Normal University, Xinyang 464000, People's Republic of China

^{62}Zhejiang University, Hangzhou 310027, People's Republic of China

^{63}Zhengzhou University, Zhengzhou 450001, People's Republic of China

Using 448.1×10^6 $\psi(3686)$ events collected with the BESIII detector at BEPCII, we employ a single-baryon tagging technique to make the first observation of $\psi(3686) \to \Xi(1530)^- \bar{\Xi}(1530)^+$ and $\Xi(1530)^- \bar{\Xi}^+$ decays with a statistical significance of more than 10σ and 5.0σ, respectively. The branching fractions are measured to be $\mathcal{B}(\psi(3686) \to \Xi(1530)^- \bar{\Xi}(1530)^+) = (11.45 \pm 0.40 \pm 0.59) \times 10^{-5}$ and $\mathcal{B}(\psi(3686) \to \Xi(1530)^- \bar{\Xi}^+) = (0.70 \pm 0.11 \pm 0.04) \times 10^{-5}$. The angular distribution parameter for $\psi(3686) \to \Xi(1530)^- \bar{\Xi}(1530)^+$ is determined to be $\alpha = 0.40 \pm 0.24 \pm 0.06$, which agrees with the theoretical predictions within 1σ. The first uncertainties are statistical, and the second systematic.

*Corresponding author.
wangxiongfei@lzu.edu.cn

^{a}Also at Bogazici University, 34342 Istanbul, Turkey.

^{b}Also at The Moscow Institute of Physics and Technology, Moscow 141700, Russia.

^{c}Also at The Functional Electronics Laboratory, Tomsk State University, Tomsk, 634050, Russia.

^{d}Also at The Novosibirsk State University, Novosibirsk 630090, Russia.

^{e}Also at The NRC "Kurchatov Institute," PNPI, 188300 Gatchina, Russia.

^{f}Also at Istanbul Arel University, 34295 Istanbul, Turkey.

^{g}Also at Goethe University Frankfurt, 60323 Frankfurt am Main, Germany.

^{h}Also at Key Laboratory for Particle Physics, Astrophysics and Cosmology, Ministry of Education; Shanghai Key Laboratory for Particle Physics and Cosmology; Institute of Nuclear and Particle Physics, Shanghai 200240, People's Republic of China.

^{i}Also at Government College Women University, Sialkot 51310, Punjab, Pakistan.

^{j}Also at Key Laboratory of Nuclear Physics and Ion-beam Application (MOE) and Institute of Modern Physics, Fudan University, Shanghai 200443, People's Republic of China.

^{k}Also at Harvard University, Department of Physics, Cambridge, Massachusetts 02138, USA.

The decays of the charmonium resonances, such as $\psi(3686)$, into baryon antibaryon pairs $(B\bar{B})$ have been extensively studied as a useful test of perturbative QCD [1,2]. They proceed via the annihilation of the $c\bar{c}$ pair into three gluons for strong decays or a virtual photon for electromagnetic decays. Within the context of SU(3) flavor symmetry, decays of charmonium to $B\bar{B}$ (i.e., $B_1\bar{B}_1$, $B_8\bar{B}_8$, and $B_{10}\bar{B}_{10}$, where B_1 is for baryon singlet, B_8 is for baryon octet, and B_{10} is for baryon decuplet) are allowed, but decays into octet-decuplet baryonic pairs $(B_{10}\bar{B}_8)$ are forbidden [3,4]. However, many experimental results on $J/\psi \to B_{10}\bar{B}_8$ decay [5,6] indicate the presence of flavor SU(3) symmetry breaking. There is no previous experimental information on $\psi(3686) \to B_{10}\bar{B}_8$, such as $\psi(3686) \to \Xi(1530)^- \bar{\Xi}^+$ decay.

Due to hadron helicity conservation [1,7], the angular distributions for the process $e^+e^- \to \psi(3686) \to B\bar{B}$ are given by

$$\frac{dN}{d\cos\theta_B} \propto 1 + \alpha\cos^2\theta_B, \qquad (1)$$

where θ_B is the angle between one of the baryons and the e^+ beam direction in the e^+e^- center-of-mass (CM) system, and the α is the angular distribution parameter,

which is widely investigated in theory and experiment [8–10]. Many theoretical models, such as those considering quark mass effects [11] and electromagnetic effects [12], predict that the angular distribution parameter obeys $\alpha < 1$. The BES and BESIII collaborations measured the angular distribution of $J/\psi \to \Sigma^0\bar{\Sigma}^0$, $\Sigma(1385)\bar{\Sigma}(1385)$ and obtained a negative α value, but with poor precision [10,13]. Chen and Ping [14] noted that the angular distribution parameter for J/ψ and $\psi(3686) \to B\bar{B}$ could be negative when rescattering effects of $B\bar{B}$ in heavy quarkonium decays are taken into account. Additional measurements of the α parameter are of interest to confront the various theoretical approaches. In other experiments, the angular distributions for charmonium decays to baryon pairs, such as J/ψ and $\psi(3686) \to p\bar{p}, \Lambda\bar{\Lambda}, \Sigma^0\bar{\Sigma}^0, \Xi\bar{\Xi}$, $\Sigma(1385)\bar{\Sigma}(1385)$ [9,15], were reported. Negative α values were found for the processes $J/\psi \to \Sigma^0\bar{\Sigma}^0$, $\Sigma(1385)\bar{\Sigma}(1385)$, while for other processes α was either measured to be positive, or not measured. The BESIII experiment has a large data sample at the $\psi(3686)$ resonance, which can be used to verify the theoretical models for the process like $\psi(3686) \to \Xi(1530)^-\bar{\Xi}(1530)^+$, for which the α value is predicted to be 0.18 and 0.31 [11,12].

In this paper, the observation of $\psi(3686) \to \Xi(1530)^-\bar{\Xi}(1530)^+$ and $\Xi(1530)^-\bar{\Xi}^+$ decays is presented based on 448.1×10^6 $\psi(3686)$ events [16] collected with the BESIII detector at the BEPCII in 2009 and 2012. Selection of $\psi(3686) \to \Xi(1530)^-\bar{\Xi}(1530)^+$ and $\Xi(1530)^-\bar{\Xi}^+$ events via full reconstruction suffers from low efficiency. To achieve a higher efficiency, we first reconstruct a $\Xi(1530)^-$, referred to as a $\Xi(1530)^-$ tag, and then search for a recoiling $\bar{\Xi}(1530)^+$ or $\bar{\Xi}^+$ signal [unless otherwise noted, charge conjugation (c.c.) is implied throughout the paper].

To determine the detection efficiencies for $\psi(3686) \to \Xi(1530)^-\bar{\Xi}(1530)^+$ and $\Xi(1530)^-\bar{\Xi}^+$, 100 000 simulated events are generated for each reconstructed mode. For the $\Xi(1530)^-\bar{\Xi}(1530)^+$ final state, the angular distribution is generated with the α value measured in this analysis, while for $\Xi(1530)^-\bar{\Xi}^+$ we use $\alpha = 1$ based on theory [17]. The $\Xi(1530)^-$ decays to the $\pi^{0(-)}\Xi^{-(0)}$ modes, with $\Xi^{0(-)} \to \pi^{0(-)}\Lambda$, $\Lambda \to p\pi^-$, and $\pi^0 \to \gamma\gamma$, are simulated using EVTGEN [18], and the response of the BESIII detector is modeled with Monte Carlo (MC) simulations using a framework based on GEANT4 [19]. A detailed description of the BESIII detector is given in Ref. [20]. To study the potential backgrounds, an inclusive MC sample of 350×10^6 $\psi(3686)$ decays is generated, where the production of the $\psi(3686)$ resonance is simulated with the KKMC generator [21], the subsequent decays are processed via EVTGEN [18] according to the measured branching fractions provided by the Particle Data Group (PDG) [22], and the remaining unmeasured decay modes are generated with LUNDCHARM [23]. Data collected at the CM energy of 3.65 GeV (off-peak data sample, 44 pb^{-1}) [16] are used to

estimate the contamination from the continuum processes $e^+e^- \to \Xi(1530)^-\bar{\Xi}(1530)^+$ and $\Xi(1530)^-\bar{\Xi}^+$.

Charged tracks are reconstructed in the main drift chamber (MDC) within an angular range of $|\cos\theta| < 0.93$, where θ is the polar angle with respect to the e^+ beam direction. Information on the specific energy deposition (dE/dx) in the MDC and from the time-of-flight (TOF) counters are combined to form particle identification (PID) confidence levels (C.L.'s) for pion, kaon, and proton hypotheses. Each track is assigned to the particle type with the highest C.L. At least two negatively charged pions and one proton are required. Photons are reconstructed from isolated showers in the electromagnetic calorimeter (EMC). Energy deposited in the nearby TOF counters is included to improve the reconstruction efficiency and energy resolution. Photon energies are required to be greater than 25 MeV in the EMC barrel region ($|\cos\theta| < 0.80$) or greater than 50 MeV in the EMC end caps ($0.86 < |\cos\theta| < 0.92$). Showers in between these angular regions are poorly reconstructed and are excluded. The EMC shower timing is required to be within the range [0, 700] ns, relative to the event start time, to suppress electronic noise and energy deposits unrelated to the analyzed event. The number of good photon candidates, N_γ, must satisfy $2 \leq N_\gamma \leq 15$ based on a simulated signal MC study.

In order to reconstruct π^0 candidates, a one-constraint (1C) kinematic fit is applied to all $\gamma\gamma$ combinations, constraining the two-photon invariant mass to the nominal π^0 mass [22]. To suppress non-π^0 backgrounds, only combinations with $\chi^2_{1C} < 20$ are retained by optimizing the figure of merit FOM $= \frac{S}{\sqrt{S+B}}$, where S is the number of signal events and B is the number of background events, based on the MC simulation. The Λ candidates are reconstructed from $p\pi^-$ pairs with an invariant mass within 5 MeV/c^2 of the nominal Λ mass. This interval is determined by optimizing the FOM. A secondary vertex fit [24] is performed on all $p\pi^-$ combinations; those with $\chi^2 < 500$ are kept for further analysis. To further suppress the background, the decay length of the Λ is required to be positive. In the case of multiple candidates, the one with an unconstrained mass closest to the nominal mass is retained as used in Ref. [13]. The Ξ candidates are reconstructed by considering all $\pi\Lambda$ combinations within 10 MeV/c^2 of the nominal Ξ mass. For Ξ^- candidates, a secondary vertex-constrained fit is used, while for both charged and neutral Ξ, only the candidate closest to the nominal mass is retained when there is more than one per event. The decay length of the Ξ^- is required to be positive to further suppress the backgrounds. The $\Xi(1530)^-$ candidates are reconstructed in the $\pi^0\Xi^-$ and $\pi^-\Xi^0$ modes and the candidate closest to the nominal mass is retained when there is more than one per event.

The antibaryon candidates $\bar{\Xi}^+$ and $\bar{\Xi}(1530)^+$ are inferred by the mass recoiling against the selected $\pi\Xi$ system,
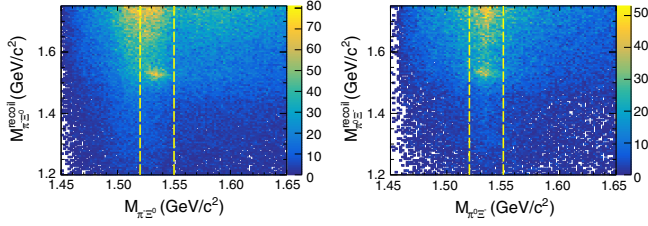
FIG. 1.   Distributions of $M_{\pi\Xi}$ versus $M_{\pi\Xi}^{\rm recoil}$ for (left panel) $\pi^-\Xi^0$ mode and (right panel) $\pi^0\Xi^-$ mode. The dashed lines denote the $\Xi(1530)$ signal region.

$$M_{\pi\Xi}^{\rm recoil} = \sqrt{(E_{\rm CM} - E_{\pi\Xi})^2 - |\vec{p}_{\pi\Xi}|^2}, \qquad (2)$$

where $E_{\pi\Xi}$ and $\vec{p}_{\pi\Xi}$ are the energy and momentum of the selected $\pi\Xi$ system, and $E_{\rm CM}$ is the CM energy. Figure 1 shows the scatterplot of $M_{\pi\Xi}$ versus $M_{\pi\Xi}^{\rm recoil}$. To determine signal yields, the mass of the $\pi\Xi$ is required to be within 15 MeV/c^2 of the nominal mass of $\Xi(1530)^-$.

Our inclusive MC sample reveals that the main background for $\psi(3686)\to\Xi(1530)^-\bar{\Xi}(1530)^+$ and $\Xi(1530)^-\bar{\Xi}^+$ decays comes from $\psi(3686) \to \pi^+\pi^-(\pi^0\pi^0)J/\psi$ with $J/\psi \to \Xi^-\bar{\Xi}^+$; it is distributed smoothly in the signal region of $M_{\pi\Xi}^{\rm recoil}$. Only a few events in the off-peak data sample survive and do not form any obvious peaking structures in the $\Xi(1530)$ signal region of the corresponding $M_{\pi\Xi}^{\rm recoil}$ distribution. Taking into account the normalization of the luminosity and CM energy dependence of the cross section, the contribution from continuum processes is expected to be small and is neglected in the further analysis. There are transition π^0's with similar momenta in both the baryon and antibaryon decay chains within the signal events. Incorrect use of these in the Ξ^0 or $\Xi(1530)^-$ reconstruction leads to a wrong combination background (WCB).

The signal yields for the two decays $\psi(3686) \to \Xi(1530)^-\bar{\Xi}(1530)^+$ and $\Xi(1530)^-\bar{\Xi}^+$ are determined by performing an extended maximum likelihood fit to the $M_{\pi\Xi}^{\rm recoil}$ spectrum. In the fit, the signal shapes for the two decays are represented by the simulated MC shape convolved with a Gaussian function to take into account the mass resolution difference between the data and the MC simulation, where the parameters of the Gaussian function are left free but are shared by the two decay modes. The WCB is described by the simulated MC shape, and the corresponding numbers of events are fixed according to the MC simulation. The other remaining backgrounds (Other-Bkg) are found to distribute smoothly in the $M_{\pi\Xi}^{\rm recoil}$ spectrum and are therefore described by a third-order Chebychev function. Figure 2 shows the $M_{\pi\Xi}^{\rm recoil}$ distributions for the $\Xi(1530)^-$ and $\bar{\Xi}(1530)^+$ tags, respectively, with Ξ and $\Xi(1530)$ peaks evident in each. Including systematic uncertainties, the significance for $\psi(3686) \to \Xi(1530)^-\bar{\Xi}^+$ is calculated to be more than 5.0σ for the $\Xi(1530)^-\bar{\Xi}$ mode and its c.c. mode combined. The individual significances are calculated from the change in log likelihood and degrees of freedom with and without the signal in the fit.

The branching fraction is calculated as

$$\mathcal{B}[\psi(3686) \to X] = \frac{N_{\rm obs}}{N_{\psi(3686)} \cdot \sum_i \epsilon_i \mathcal{B}_i}, \qquad (3)$$

where X stands for $\Xi(1530)^-\bar{\Xi}(1530)^+$ or $\Xi(1530)^-\bar{\Xi}^+$, $N_{\rm obs}$ is the number of extracted signal events, $N_{\psi(3686)}$ is the total number of $\psi(3686)$ events [16], i runs over the $\pi^-\Xi^0$ and $\pi^0\Xi^-$ modes, ϵ_i denotes the detection efficiency obtained with the measured α value for both modes, and $\mathcal{B}_i$ denotes the product of branching fractions of
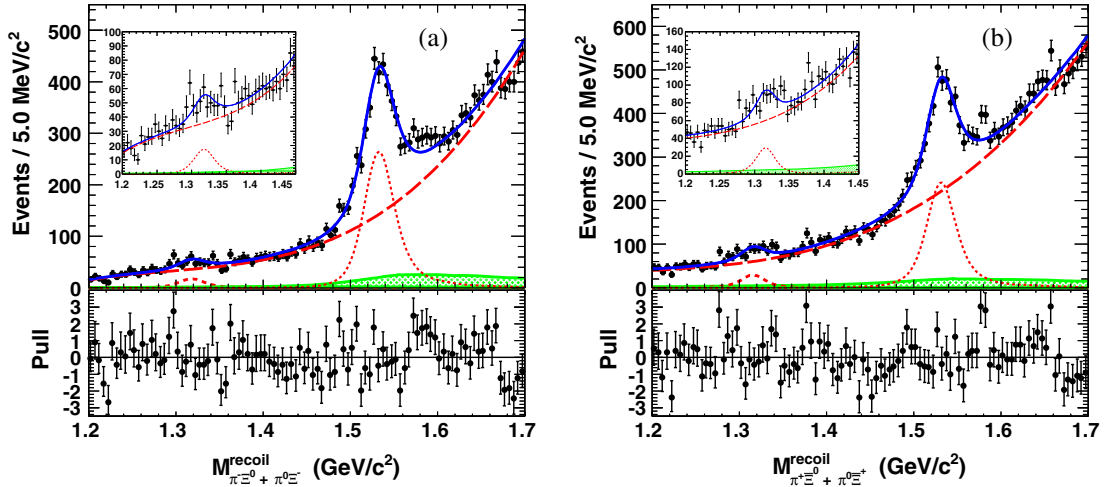

FIG. 2.   Fit to recoil mass spectra of (a) $M_{\pi^-\Xi^0+\pi^0\Xi^-}^{\rm recoil}$ and (b) $M_{\pi^+\bar{\Xi}^0+\pi^0\bar{\Xi}^+}^{\rm recoil}$. Dots with error bars are for data, the blue solid lines show the fit result, the red short-dashed lines are for signal, the red long-dashed ones are for the smooth background (Other-Bkg), and the green hatched ones are for the WCB. (Insets) The $\bar{\Xi}^+$ signal region in more detail.

TABLE I. The number of the extracted events (N_{obs}), efficiencies (ϵ_1 is for $\pi^-\Xi^0$ mode, ϵ_2 is for $\pi^0\Xi^-$ mode), statistical significance (S), the angular distribution parameter (α), and branching fractions ($\mathcal{B}$), where $\mathcal{B}^{com}$ and α^{com} denote the combined branching fraction and angular distribution parameters. The first uncertainties are statistical, and the second systematic.

Tag mode	$\psi(3686) \to \Xi(1530)^-\bar{\Xi}(1530)^+$		$\psi(3686) \to \Xi(1530)^-\bar{\Xi}^+$	
	$\Xi(1530)^-$	$\bar{\Xi}(1530)^+$	$\Xi(1530)^-$	$\bar{\Xi}(1530)^+$
N_{obs}	2664 ± 114	2403 ± 132	152 ± 37	247 ± 48
ϵ_1 (%)	7.85 ± 0.09	7.16 ± 0.08	8.89 ± 0.09	8.42 ± 0.09
ϵ_2 (%)	8.91 ± 0.09	8.17 ± 0.09	10.58 ± 0.10	9.82 ± 0.10
$S(\sigma)$	23.0	18.2	4.4	5.3
α	$0.43 \pm 0.30 \pm 0.09$	$0.36 \pm 0.35 \pm 0.08$	$\cdots$	$\cdots$
$\mathcal{B}(10^{-5})$	$11.51 \pm 0.49 \pm 0.92$	$11.36 \pm 0.62 \pm 1.14$	$0.57 \pm 0.14 \pm 0.05$	$0.93 \pm 0.18 \pm 0.10$
α^{com}	$0.40 \pm 0.24 \pm 0.06$		$\cdots$	
$\mathcal{B}^{com}(10^{-5})$	$11.45 \pm 0.40 \pm 0.59$		$0.70 \pm 0.11 \pm 0.04$	

$\Xi(1530) \to \pi\Xi$ and $\Xi \to \pi\Lambda$. Table I summarizes the numerical results for the various modes studied. The angular distribution parameter for $\psi(3686) \to \Xi(1530)^-\bar{\Xi}(1530)^+$ decay is determined by performing a least squares fit to the $\cos\theta_B$ distribution in the range from -0.8 to 0.8 by Eq. (1), divided into eight equidistant intervals; this is done separately for $\Xi(1530)^-$ and $\bar{\Xi}(1530)^+$ tags. The signal yield in each $\cos\theta_B$ bin is obtained with the aforementioned fit method in the $M_{\pi\Xi}^{recoil}$ range of 1.4 GeV/c^2 to 1.7 GeV/c^2. The distributions of the efficiency-corrected signal yields together with the fit curves are shown in Fig. 3. The α values obtained are summarized in Table I.

Systematic uncertainties on the branching fraction measurements are mainly due to differences of detection efficiency between data and MC simulation. The uncertainties associated with the efficiencies of tracking and PID for the pion from the mother particle $\Xi(1530)^-$ in the $\pi^-\Xi^0$ decay mode are investigated with the control sample $J/\psi \to p\bar{p}\pi^+\pi^-$. The uncertainty due to the 1C kinematic fit for the π^0 reconstruction is estimated with the control sample $J/\psi \to \rho\pi$. The uncertainties related to the Ξ^0 and Ξ^- reconstruction efficiency combined with tracking, PID, and the Λ reconstruction efficiencies are estimated using the control sample $\psi(3686) \to \Xi^0\bar{\Xi}^0$ and $\Xi^-\bar{\Xi}^+$. A detailed description of our methods can be found in Refs. [13,25].
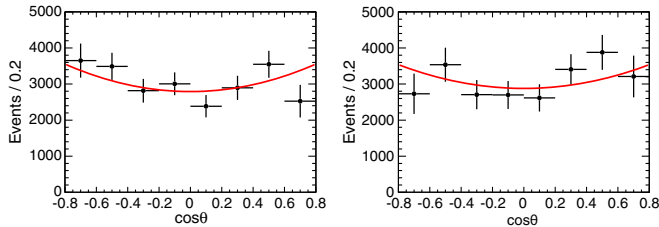

FIG. 3. Distributions of $\cos\theta_B$ for (left panel) the $\Xi(1530)^-$ tag and (right panel) the $\bar{\Xi}(1530)^+$ tag. The dots with error bars indicate the efficiency-corrected data, and the curves show the fit results.

The uncertainties due to the requirements for mass window and decay length of Ξ, Λ are estimated with the control sample $J/\psi \to \Xi^0\bar{\Xi}^0$ and $\Xi^-\bar{\Xi}^+$. The uncertainty related to the mass window of $\Xi(1530)^-$ is estimated by varying the half-width of 15 MeV/c^2 by ± 1 MeV/c^2. The largest difference of the efficiency between data and MC simulation is taken as the systematic uncertainty. The uncertainty due to the signal shape is estimated by changing the nominal signal function to the Breit-Wigner function; the difference of the signal yields is taken as the systematic uncertainty. The parameters of the Gaussian signal function for the $\Xi(1530)^-\bar{\Xi}^+$ final state are fixed in the fit; uncertainties are estimated by varying the nominal values by 1σ. The uncertainty due to the $M_{\pi\Xi}^{recoil}$ fitting range is estimated by varying the mass range by ± 10 MeV/c^2. The uncertainties due to the assumed polynomial background shape are estimated by alternate fits using a second- or a fourth-order Chebychev function. The uncertainty due to the WCB is estimated by comparing the signal yields between the fits with and without the corresponding component included in the fit. The uncertainty related with the detection efficiency due to the modeling of the angular distribution of the baryon pairs, represented by the parameter α, is estimated for the $\Xi(1530)^-\bar{\Xi}(1530)^+$ mode by varying the measured α values by 1σ in the MC simulation. For the $\Xi(1530)^-\bar{\Xi}^+$ mode, α is set to zero. The uncertainties due to the branching fractions of the intermediate states, $\Xi \to \pi\Lambda$ and $\Lambda \to p\pi$, are taken to be 0.1% and 0.8% according to the PDG [22]. The uncertainty of the branching fraction of $\Xi(1530) \to \pi\Xi$ is taken conservatively according to the branching fraction of $\Xi(1530) \to \gamma\Xi$, 4.0% from the PDG [22]. The uncertainties due to the total number of $\psi(3686)$ events ($N_{\psi(3686)}$) are determined with inclusive hadronic $\psi(3686)$ decays [16]. The various systematic uncertainties on the branching fraction measurements are summarized in Table II. The total systematic uncertainty is obtained by summing the individual contributions in quadrature.

Systematic issues for the measurement of the α include the determinations of signal yields in $\cos\theta_B$ intervals and

TABLE II. Systematic uncertainties (in %) and their sources for each measured decay mode.

Source	$\Xi(1530)^-\bar{\Xi}(1530)^+$		$\Xi(1530)^-\bar{\Xi}^+$	
	$\Xi(1530)^-$	$\bar{\Xi}(1530)^+$	$\Xi(1530)^-$	$\bar{\Xi}(1530)^+$
Tracking for pion	1.0	1.0	1.0	1.0
PID for pion	1.0	1.0	1.0	1.0
π^0 reconstruction	1.0	1.0	1.0	1.0
Ξ^0 reconstruction	2.6	4.8	2.6	4.8
Ξ^- reconstruction	3.0	6.0	3.0	6.0
Mass window of Λ	0.1	0.3	0.1	0.3
Decay length of Λ	0.2	0.1	0.2	0.1
Ξ^0 mass window	1.4	1.8	1.4	1.8
Ξ^- mass window	1.0	1.0	1.0	1.0
$\Xi(1530)^-$ mass window	1.0	1.0	1.0	1.0
Signal shape	2.0	2.2	1.0	1.0
Parametrization	1.0	1.0	$\cdots$	$\cdots$
Fitting range	1.8	2.0	5.0	4.9
Background shape	1.7	1.3	4.5	2.0
Wrong combinations	3.3	2.0	1.0	1.0
Angular distribution	1.0	1.0	2.3	2.5
$\mathcal{B}(\Lambda \to p\pi)$	0.8	0.8	0.8	0.8
$\mathcal{B}(\Xi(1530) \to \pi\Xi)$	4.0	4.0	4.0	4.0
$N(\psi(3686))$	0.7	0.7	0.7	0.7
Total	8.0	10.0	9.6	11.1

the $\cos\theta_B$ fitting procedure. Signal yield systematic uncertainties arise from the fit range, the background shape, signal shape, and WCB. These are evaluated with a method similar to the one described above; the resulting differences with respect to the nominal α values are taken as systematic uncertainties. The $\cos\theta_B$ fitting uncertainties are estimated by refitting the $\cos\theta_B$ distribution with a different binning and fit range. We divide $\cos\theta_B$ into five intervals instead of eight, and the change in α is taken as the systematic uncertainty. We also repeat the fit after altering the $\cos\theta_B$ range to $[-0.9, 0.9]$ or $[-0.7, 0.7]$, with the same bin size as the nominal fit. The largest changes of α with respect to the nominal fit are taken as systematic uncertainties. All the systematic uncertainties for the α measurement are summarized in Table III, where the total systematic uncertainty is the quadratic sum of the contributions.

TABLE III. Systematic uncertainties (absolute) on the measurement of α value for $\psi(3686) \to \Xi(1530)^-\bar{\Xi}(1530)^+$ decay.

Source	$\Xi(1530)^-$	$\bar{\Xi}(1530)^+$
$M_{\pi\Xi}^{\text{recoil}}$ fitting range	0.05	0.02
Background shape	0.03	0.02
Signal shape	0.06	0.04
Wrong combinations	0.01	0.04
$\cos\theta_B$ binning	0.02	0.01
$\cos\theta_B$ fitting range	0.03	0.04
Total	0.09	0.08

Combined branching fractions and α values are calculated according to the unconstrained averaging introduced by the PDG [22]. Note that the single-baryon recoil mass method leads to some double counting of the $\Xi(1530)^-\bar{\Xi}(1530)^+$ final state; MC studies indicate this occurs at a rate of about 10%. This is taken into account when combining branching fractions and angular distribution parameters. The systematic uncertainties are weighted to properly account for common and uncommon systematic uncertainties using $\frac{1}{2}\sum_{i,j(i\neq j)} \frac{\sigma_i'\sigma_j}{\sqrt{\sigma_i'^2+\sigma_j^2}}$, where σ (σ') is the systematic uncertainty with (without) common sources, and i, j run over the baryon and antibaryon tags.

In summary, using 448.1×10^6 $\psi(3686)$ events collected with the BESIII detector at the BEPCII, we present the observation of $\psi(3686) \to \Xi(1530)^-\bar{\Xi}(1530)^+$ and $\Xi(1530)^-\bar{\Xi}^+$ decays with the statistical significances of more than 10σ and 5.0σ, respectively, based on a single-baryon tagging strategy. The branching fractions for $\psi(3686) \to \Xi(1530)^-\bar{\Xi}(1530)^+$ and $\Xi(1530)^-\bar{\Xi}^+$ are measured to be $(11.45 \pm 0.40 \pm 0.59) \times 10^{-5}$ and $(0.70 \pm 0.11 \pm 0.04) \times 10^{-5}$, where the first (second) uncertainty is statistical (systematic). The corresponding results are summarized in Table I. The observation of the decay $\psi(3686) \to \Xi(1530)^-\bar{\Xi}^+$ indicates that the SU(3) flavor symmetry is still broken in the $\psi(3686)$ case, which further validates the generality of SU(3) flavor symmetry breaking. The measured angular distribution parameter α for $\psi(3686) \to \Xi(1530)^-\bar{\Xi}(1530)^+$ decay agrees with the theoretical prediction [11,12] with our current errors. This offers support, within our limited statistics, for these models which include quark mass and electromagnetic effects.

[1] S. J. Brodsky and G. P. Lepage, Phys. Rev. D **24**, 2848 (1981).

[2] J. Bolz and P. Kroll, Eur. Phys. J. C **2**, 545 (1998); R. G. Ping, H. C. Chiang, and B. S. Zou, Phys. Rev. D **66**, 054020 (2002).

[3] D. M. Asner *et al.*, Int. J. Mod. Phys. A **24**, 499 (2009).

[4] L. Köpke and N. Wermes, Phys. Rep. **174**, 67 (1989); H. Kowalski and T. F. Walsh, Phys. Rev. D **14**, 852 (1976).

[5] M. W. Eaton *et al.*, Phys. Rev. D **29**, 804 (1984); P. Henrard *et al.* (DM2 Collaboration), Nucl. Phys. **B292**, 670 (1987).

[6] M. Ablikim *et al.* (BESIII Collaboration), Phys. Rev. D **87**, 052007 (2013).

[7] A. Pais, Phys. Rev. Lett. **26**, 51 (1971); P. Kessler, Nucl. Phys. **B15**, 253 (1970); X. Wang, B. Li, Y. Gao, and X. Lou, Nucl. Phys. **B941**, 861 (2019).

[8] F. Murgia and M. Melis, Phys. Rev. D **51**, 3487 (1995); A. Buzzo *et al.* (Fermilab E835 Collaboration), Phys. Lett. B **610**, 177 (2005).

[9] J. Z. Bai *et al.* (BES Collaboration), Phys. Lett. B **591**, 42 (2004).

[10] M. Ablikim *et al.* (BES Collaboration), Phys. Lett. B **632**, 181 (2006).

[11] C. Carimalo, Int. J. Mod. Phys. A **02**, 249 (1987).

[12] M. Claudson, S. L. Glashow, and M. B. Wise, Phys. Rev. D **25**, 1345 (1982).

[13] M. Ablikim *et al.* (BESIII Collaboration), Phys. Rev. D **93**, 072003 (2016); Phys. Lett. B **770**, 217 (2017).

[14] H. Chen and R. G. Ping, Phys. Lett. B **644**, 54 (2007).

[15] M. Ablikim *et al.* (BES Collaboration), Phys. Lett. B **648**, 149 (2007); Chin. Phys. C **36**, 1031 (2012); M. Ablikim *et al.* (BESIII Collaboration), Phys. Rev. D **95**, 052003 (2017); **98**, 032006 (2018); Nat. Phys. **15**, 631 (2019).

[16] M. Ablikim *et al.* (BESIII Collaboration), Chin. Phys. C **42**, 023001 (2018).

[17] C. Y. Pang and R. G. Ping, Chin. Phys. Lett. **24**, 1441 (2007).

[18] R. G. Ping, Chin. Phys. C **32**, 599 (2008); D. J. Lange, Nucl. Instrum. Methods Phys. Res., Sect. A **462**, 152 (2001).

[19] S. Agostinelli *et al.* (GEANT4 Collaboration), Nucl. Instrum. Methods Phys. Res., Sect. A **506**, 250 (2003); J. Allison *et al.*, IEEE Trans. Nucl. Sci. **53**, 270 (2006).

[20] M. Ablikim *et al.* (BESIII Collaboration), Nucl. Instrum. Methods Phys. Res., Sect. A **614**, 345 (2010).

[21] S. Jadach, B. F. L. Ward, and Z. Was, Comput. Phys. Commun. **130**, 260 (2000); Phys. Rev. D **63**, 113009 (2001).

[22] M. Tanabashi *et al.* (Particle Data Group), Phys. Rev. D **98**, 030001 (2018).

[23] J. C. Chen, G. S. Huang, X. R. Qi, D. H. Zhang, and Y. S. Zhu, Phys. Rev. D **62**, 034003 (2000).

[24] M. Xu *et al.*, Chin. Phys. C **33**, 428 (2009).

[25] M. Ablikim *et al.* (BESIII Collaboration), Phys. Rev. D **87**, 032007 (2013).